iScience

Article

Single-cell and spatial transcriptomics reveal pre-metastatic subsets and therapeutic targets in penile carcinoma

Graphical abstract

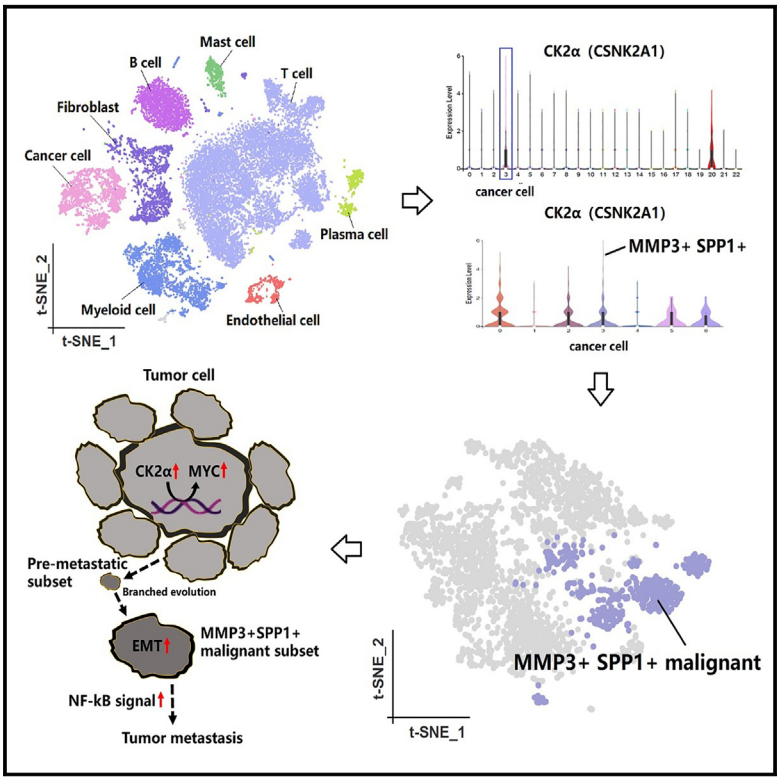

Highlights

- Upregulated CK2α can mediate the activation of oncogenes and lead to tumorigenesis
- The MMP3+SPP1+ malignant subset has a robust metastatic capability within tumors
- CK2α represents a potential target of vulnerability in penile carcinoma

Authors

Da-Ming Xu, Ling-Xiao Chen, Hui Han, Miao Mo

Correspondence

hanhui@sysucc.org.cn (H.H.), momiao@hotmail.com (M.M.)

In brief

Cancer; Omics; Transcriptomics

Xu et al., 2025, iScience *28*, 111765
February 21, 2025
https://doi.org/10.1016/j.isci.2025.111765

CellPress

iScience

CellPress
OPEN ACCESS

Article

Single-cell and spatial transcriptomics reveal pre-metastatic subsets and therapeutic targets in penile carcinoma

Da-Ming Xu,[1,2,4] Ling-Xiao Chen,[3,4] Hui Han,[1,2,*] and Miao Mo[3,5,*]
[1]State Key Laboratory of Oncology in South China, Guangdong Provincial Clinical Research Center for Cancer, Sun Yat-sen University Cancer Center, Guangzhou 510060, P.R. China
[2]Department of Urology, Sun Yat-sen University Cancer Center, Guangzhou 510060, P.R. China
[3]Department of Urology, Xiangya Hospital, Central South University, Changsha 410008, P.R. China
[4]These authors contributed equally
[5]Lead contact
*Correspondence: hanhui@sysucc.org.cn (H.H.), momiao@hotmail.com (M.M.)
https://doi.org/10.1016/j.isci.2025.111765

SUMMARY

Tumor heterogeneity, driven by branching evolution and genomic mutations, complicates cancer treatment. Understanding malignant cell evolution across various tumors aids in identifying pre-metastatic subpopulations for optimized therapies. Using bulk RNA sequencing (6 primary penile carcinomas, 6 metastatic lymph nodes, GSE196978), single-cell RNA sequencing (4 advanced penile carcinomas), spatial transcriptomics (Squamous cell carcinoma [SCC]: GSE144239-GSM4565823 and SCC: GSE144239-GSM4565826), and cell assays with Silmitasertib, we mapped heterogeneity and pinpointed therapeutic targets. In penile carcinoma, we discovered an MMP3+SPP1+ pre-metastatic subset and casein kinase 2 alpha 1 (CK2α) overexpression. The nuclear factor κB (NF-κB) pathway may drive metastasis. Pan-cancer analysis showed that MMP3 and SPP1 link to epithelial mesenchymal transition (EMT) and drug resistance, while CK2α activates oncogenes. Silmitasertib, a CK2α inhibitor, exhibited anti-tumor effects in penile carcinoma cells. Validated across 98 single-cell and 6 spatial datasets, our study advances the understanding of tumorigenesis and metastasis, highlighting Silmitasertib as a potential therapeutic agent.

INTRODUCTION

The branching evolution and genomic mutations of tumor cells give rise to intratumor heterogeneity within solid tumors.[1] Researching intratumor heterogeneity aids in deeper comprehending the complexity of tumor cell clonality and in distinguishing pre-metastatic malignant cell subpopulations, marking a significant breakthrough in the study of tumor metastasis.[2,3]

Penile carcinoma is a rare genitourinary tumor, and, currently, we have limited understanding of its intratumor heterogeneity. Lymph node metastasis is unequivocally linked to a poor prognosis in penile carcinoma.[4,5] Theoretically, identifying and targeting malignant subpopulations of penile carcinoma cells with metastatic and drug-resistant properties can reduce tumor growth and spread, significantly improving patient prognosis. Additionally, these metastatic markers may also be applicable to other tumor systems.

Recent studies have highlighted the significant roles of matrix metalloproteinase 3 (MMP3) and secreted phosphoprotein 1 (SPP1) in tumor progression. MMP3, in particular, is recognized for its critical involvement in tumor progression, as it degrades extracellular matrix (ECM) components, thereby facilitating the invasion and metastasis of tumor cells.[6,7] Concurrently, SPP1, also known as osteopontin, is a glycoprotein that plays a key role in ECM remodeling and cell migration.[8] Given the interplay between MMP3 and SPP1 in driving changes in the tumor microenvironment and enhancing metastasis, further investigation into their distribution and function in malignant components will be essential for deepening our understanding of the mechanisms underlying disease progression.

Casein kinase 2 alpha 1 (CK2α) is an important protein kinase involved in phosphorylation, playing a crucial role in tumor.[9] CK2α is involved in regulating multiple cellular signaling pathways, including processes such as cell proliferation, apoptosis, and DNA repair.[10] Previous studies indicated that dysregulation of the CK2α alpha subunit expression could endow cells with carcinogenic potential and significantly enhance the tumor phenotype in collaboration with oncogenes.[11,12]

Hence, the objective of our study was to expand our research from rare penile carcinoma to other tumor systems, identifying MMP3+SPP1+ as a pre-metastatic subpopulation of malignant cells and CK2α as a switch for tumorigenesis at both spatial and single-cell resolution. Given the limitations of existing research, our findings offer significant insights for developing therapeutic

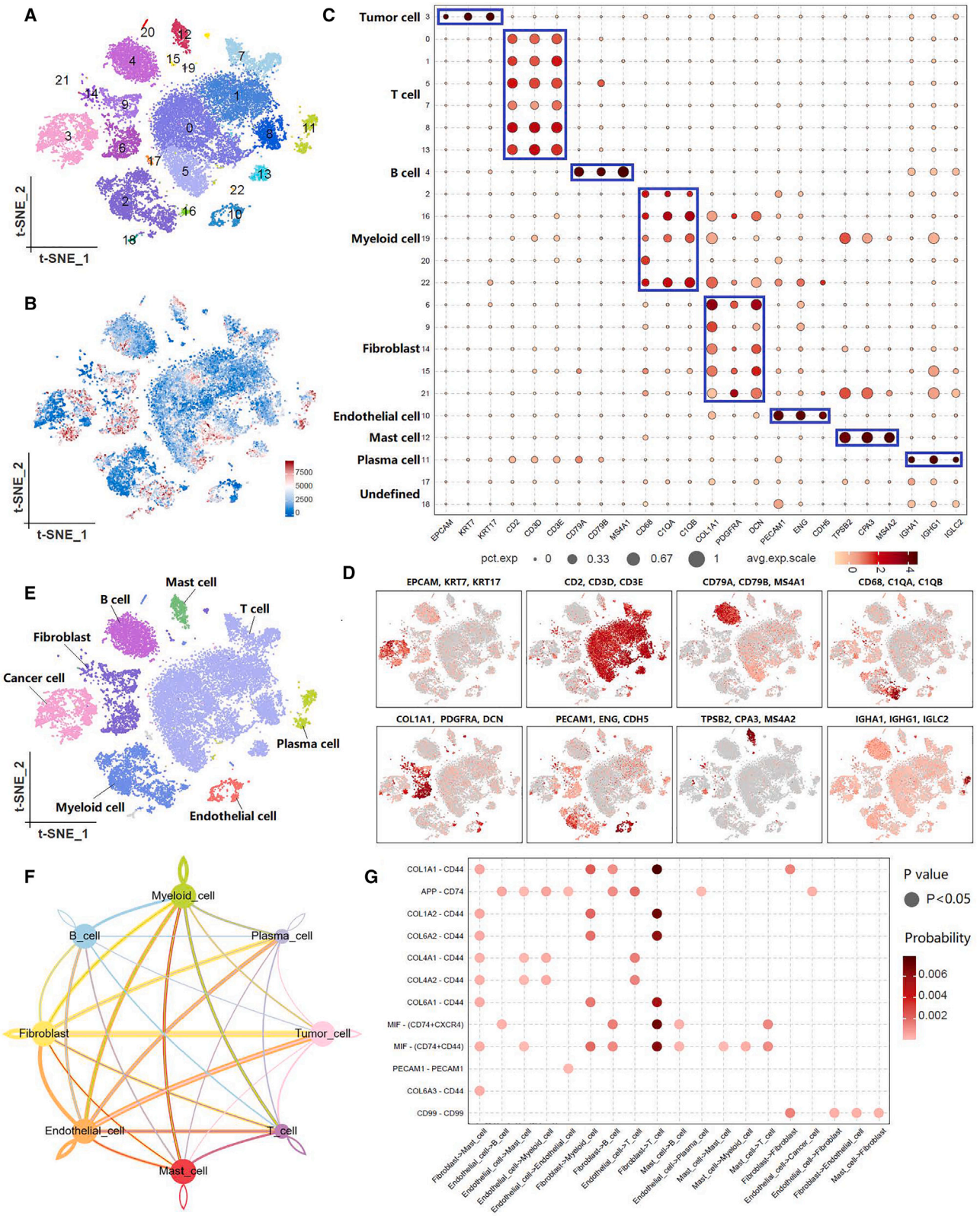

(legend on next page)

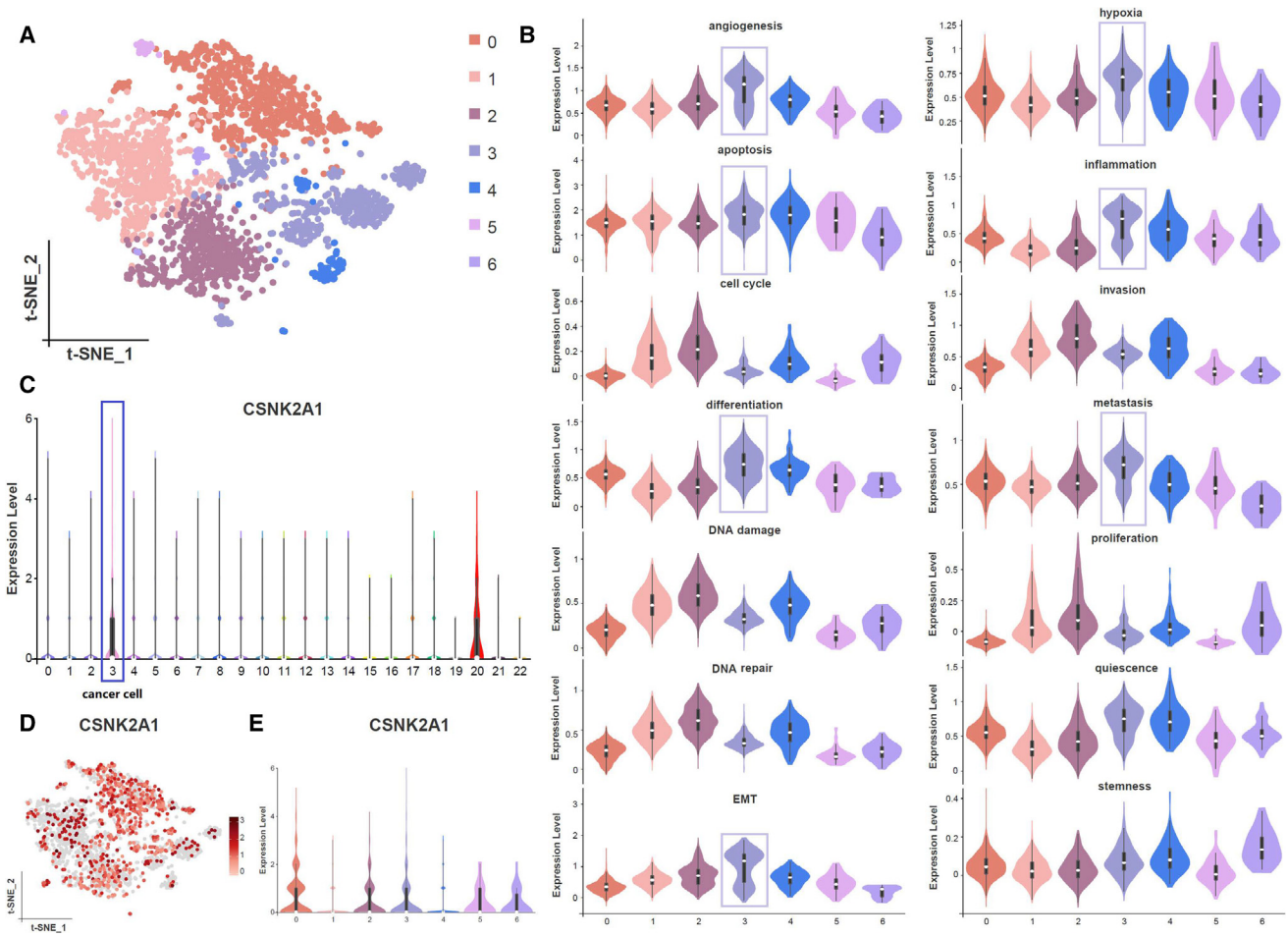

Figure 2. Tumor cell re-clustering and cell status evaluation

(A) t-SNE plots of 7 distinct clusters of malignant cells.

(B) Cellular functionalities of distinct malignant cell subsets.

(C) The expression level of CSNK2A1 across all cell clusters.

(D and E) The expression level of CSNK2A1 in various malignant subsets.

All data are represented as mean ± SD.

strategies targeting CK2α and hold promise for guiding approaches to personalized treatment for rare genitourinary or metastatic tumors.

RESULTS

Single-cell landscapes of penile carcinoma

Single-cell landscapes of four penile carcinoma single-cell datasets unveiled a total of 25,712 cells, with an average of 6,428 cells per sample, distributed across 22 distinct clusters (Figure 1A). The unique molecular identifier (UMI) tags in single-cell transcriptomic information revealed the diversity in gene expression levels among individual cells (Figure 1B). By manually annotating the cells, the single-cell data were categorized into eight cell components, namely tumor cell (EPCAM, KRT7, KRT17), T cell (CD2, CD3D, CD3E), B cell (CD79A, CD79B, MS4A1), myeloid cell (CD68, C1QA, C1QB), fibroblast (COL1A1, PDGFRA, DCN), endothelial cell (PECAM1, ENG, CDH5), mast cell (TPSB2, CPA3, MS4A2), and plasma cell (IGHA1, IGHG1, IGLC2) (Figures 1C–1E). Cell communication analysis was used to indicate interaction network among all cell components and predict signaling pathways between ligand and receptor (Figures 1F and 1G).

Figure 1. Single-cell landscapes of advanced penile carcinoma

(A) t-Distributed Stochastic Neighbor Embedding (t-SNE) plots of 22 distinct single-cell clusters in penile carcinoma.

(B) UMI tags in single-cell transcriptomic information.

(C–E) The main cell types manually annotated by known cell lineages.

(F) Cell interaction network among all cell components in tumor microenvironment of penile carcinoma.

(G) Signaling pathways between ligand and receptor.

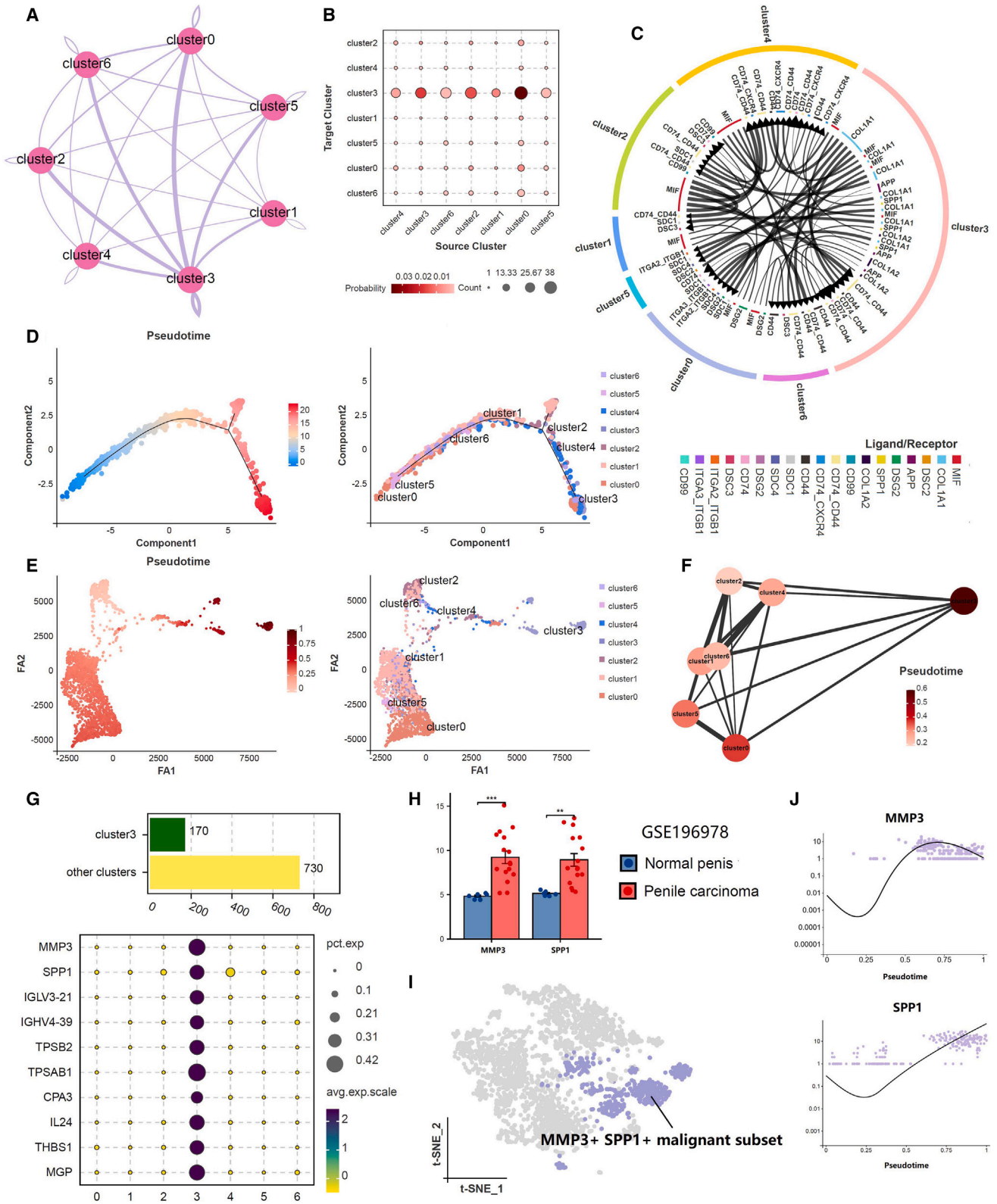

(legend on next page)

Tumor cell re-clustering and cell status evaluation

The malignant cells were re-clustered using Seurat via the Shared Nearest Neighbor (SNN) clustering algorithm, leading to the identification of 7 distinct clusters of malignant cells (Figure 2A). Due to the stringent ethical constraints associated with procuring normal penile tissue, this study exclusively collected penile carcinoma samples, all pathologically confirmed to be malignant squamous cell carcinoma. The absence of normal tissue limits the utility of Inference of Copy Number Variations (InferCNV) for identifying malignant cells. Therefore, we employed tumor hallmarks-based validation to further assess the cellular functionalities of distinct inferred malignant cell subgroups, aiming to identify the most potentially metastatic malignant cells.[13,14] Obviously, cluster 3 exhibited remarkable abilities in angiogenesis, epithelial mesenchymal transition (EMT), and metastasis (Figure 2B). Based on these findings, we inferred that it represents a pre-metastatic malignant subgroup. Additionally, the expression level of CSNK2A1 (the encoding gene for CK2α) in tumor cells was high across all cell types (Figure 2C), with elevated expression levels observed in various malignant subgroups, particularly clusters 0, 2, 3, 5, and 6 (Figures 2D and 2E). Our research indicated that malignant cells exhibited a high level of phosphorylation, which could be linked to the aberrant activation of malignant cell phenotypes and functions.

Interaction analysis, trajectory analysis, and identification of cluster 3

Cell communication analysis was reflected through network diagrams and bubble plots, highlighting the distinctiveness of cluster 3 (Figures 3A and 3B). The signal pathway strength emanating from cluster 3 is the most pronounced, indicating its close relationship with other clusters and its dominant position. The ligand-receptor network diagram further unveiled potential signaling pathways among cell clusters and also emphasized the dominant advantage of cluster 3 within these pathways (Figure 3C). Both pseudo-time trajectory and partition-based graph abstraction (PAGA) trajectory indicated that cluster 3 emerged as a subgroup in the later stages of tumor heterogeneity evolution, as a consequence of continuous cellular clonal expansion and branching evolution (Figures 3D–3F). The upregulated gene analysis suggested that cluster 3 manifested a total of 170 upregulated genes in contrast to other clusters (Figure 3G). We have curated the top 10 genes and confirmed their expression patterns across the 7 clusters via a bubble plot. We further utilized the GSE196978 dataset to verify the expression of upregulated genes in cluster 3 across both penile carcinoma and normal tissues (Figure 3H). Based on these findings, we defined cluster 3 as MMP3+SPP1+ malignant subset (Figure 3I). Single-cell trajectory analysis similarly confirmed that MMP3 and SPP1 emerged in the later stages of pseudo-time (Figure 3J).

Distinguishing functional differences between MMP3+SPP1+ malignant subset and other clusters

Kyoto Encyclopedia of Genes and Genomes (KEGG) enrichment analysis revealed distinct signaling pathways between MMP3+SPP1+ malignant subset and other clusters. MMP3+SPP1+ malignant subset mainly involved in the NF-κB signaling pathway and Toll-like receptor signaling pathway, while "other clusters" group was associated with the p53 signaling pathway (Figures 4A and 4B). Importantly, functional enrichment analysis also suggested a critical role for proteoglycans in cancer. Proteoglycans served as pivotal mediators in the interactions between cells and the extracellular microenvironment, closely intertwined with the remodeling of the ECM.[15] Additionally, Gene Ontology (GO) enrichment analysis similarly indicated significant ECM remodeling in the MMP3+SPP1+ malignant subset, which may serve as a key foundation for mediating the invasion and metastasis of penile tumor cells (Figures 4C and 4D). Cell communication analysis among MMP3+SPP1+ malignant subset and other immune cell subtypes suggested that fibroblast in the microenvironment was closely linked to the MMP3+SPP1+ malignant subset, where Amyloid Precursor Protein (APP)-CD74 signal may be the key pathway (Figures 4E, 4F, and S1). Squamous cell carcinoma spatial transcriptomics data revealed that MMP3 and SPP1 were located in malignant area and were positively correlated with tumor cells (Figures 4G and 4H). The pathway disturbance analysis in pan-cancer suggested that high levels of MMP3 or SPP1 were associated with the upregulation of the NF-κB pathway (Figures 4I and 4J). Based on the aforementioned findings, we inferred that the MMP3+SPP1+ malignant subset represented a pre-metastatic subpopulation in penile carcinoma.

Distinguishing pathway differences between metastatic lymph nodes and primary penile carcinoma

We collected 12 tumor samples from 6 advanced-stage penile carcinoma patients, including 6 pairs of matched samples of metastatic lymph nodes and primary lesions. Through bulk RNA sequencing (bulk RNA-seq), we analyzed the genomic characteristics and signaling pathway differences between metastatic lesions and primary lesions (Figure 5A). Certainly, there were distinct differences in the gene expression patterns between metastatic lymph nodes and primary penile carcinoma (Figures 5B and 5C). It was noteworthy that the gene set

Figure 3. The distinctiveness and identification of cluster 3

(A and B) Cell communication analysis of different malignant clusters in penile carcinoma.

(C) The ligand-receptor network diagram of potential signaling pathways among cell clusters.

(D) Pseudo-time trajectory of all malignant cell clusters.

(E and F) PAGA trajectory of all malignant cell clusters.

(G) The upregulated gene analysis of cluster 3 and other clusters.

(H) The expression of MMP3 and SPP1 in the GSE196978 dataset. *$p < 0.05$, **$p < 0.01$, ***$p < 0.001$, ****$p < 0.0001$. Data are represented as mean ± SD.

(I) The identification of cluster 3.

(J) Single-cell trajectory analysis of MMP3 and SPP1.

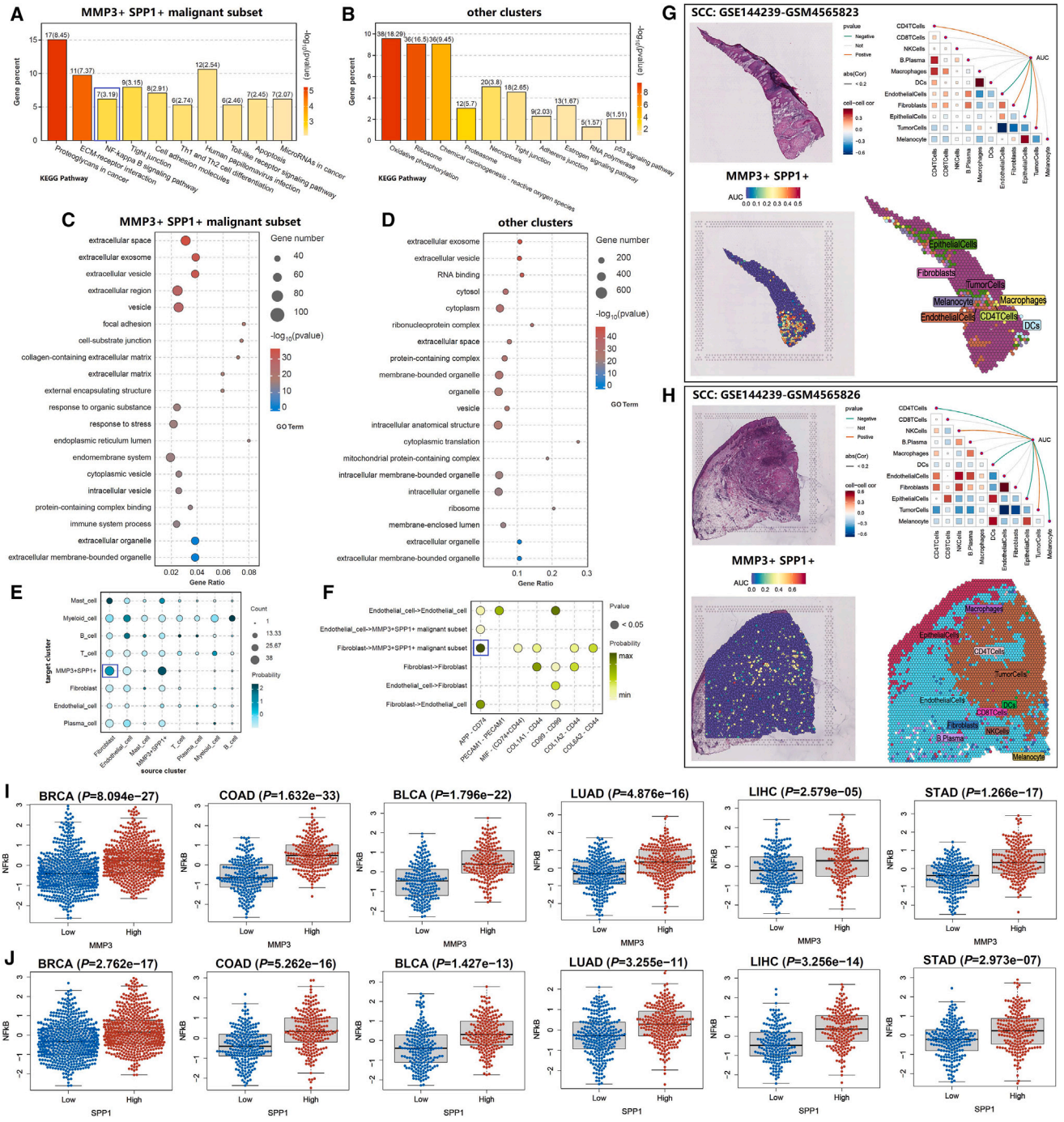

Figure 4. Functional differences between MMP3+SPP1+ malignant subset and other clusters

(A and B) KEGG enrichment analysis of MMP3+SPP1+ malignant subset and other clusters.

(C and D) GO enrichment analysis of MMP3+SPP1+ malignant subset and other clusters.

(E) Cell communication analysis among MMP3+SPP1+ malignant subset and other immune cell subtypes.

(F) Signaling pathways between ligand and receptor.

(G and H) The spatial transcriptomic expression localization and expression correlation of MMP3+SPP1+ in squamous cell carcinoma.

(I and J) The impact of high- and low-expression groups of MMP3 and SPP1 on the NF-κB signaling pathway.

Data are represented as mean ± SD.

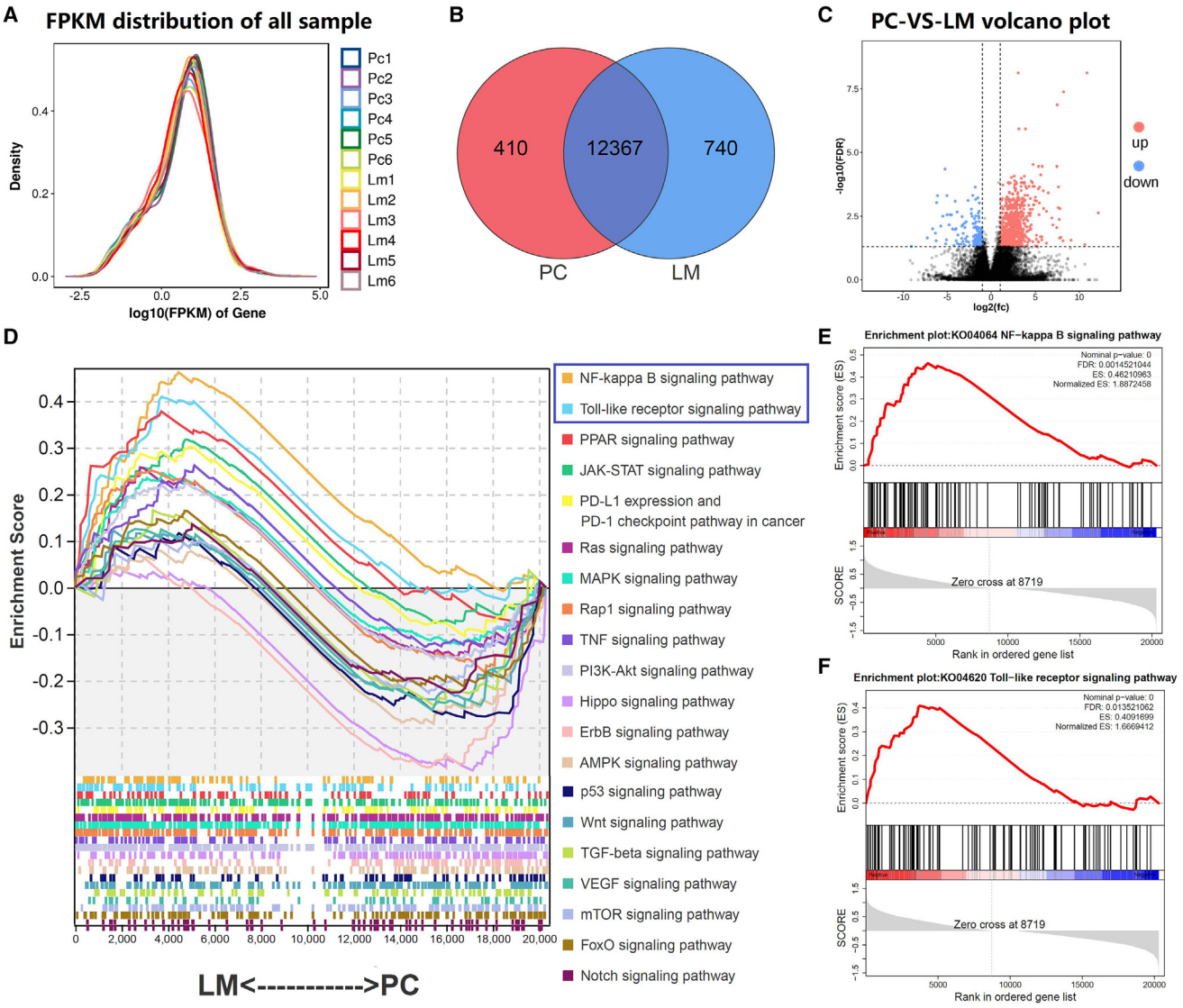

Figure 5. The differences between metastatic lymph nodes and primary penile carcinoma

(A) Fragments Per Kilobase of exon per Million fragments mapped (FPKM) distribution of 12 samples.

(B) Venn diagram of gene expression.

(C) Volcano plot of gene expression.

(D) GSEA enrichment analysis covered 20 signaling pathways.

(E and F) Enrichment plot of the NF-κB signaling pathway and Toll-like receptor signaling pathway.

enrichment analysis (GSEA) enrichment analysis covered 20 signaling pathways, indicating that the activation of the NF-κB signaling pathway and Toll-like receptor signaling pathway was primarily involved in the metastatic lesion (Figures 5D–5F). This was consistent with the signaling pathways enriched in the MMP3+SPP1+ malignant subset that we observed previously. The NF-κB signaling pathway and Toll-like receptor signaling pathway were both considered critical avenues for facilitating tumor metastasis.[16,17] Our discoveries within the metastatic lesions reiterated the likelihood of the MMP3+ SPP1+ malignant subset being the driving force behind tumor metastasis.

Validating the participation of MMP3 and SPP1 in cell status and drug sensitivity across various tumor types

In multiple tumor types, MMP3 and SPP1 were frequently overexpressed in the tumor group, and knockout experiments conducted across various tumor cell lines via CRISPR-Cas9 simulations indicated that inhibiting MMP3 or SPP1 can effectively suppress cell growth (Figure S2). These findings underscored the potential of MMP3 and SPP1 as promising targets for tumor therapy. Crucially, the expression levels of MMP3 and SPP1 showed a significant positive correlation with the EMT, metastasis, and invasion processes in tumor, further substantiating their roles in facilitating tumor cell dissemination (Figures 6A and 6B). Importantly,

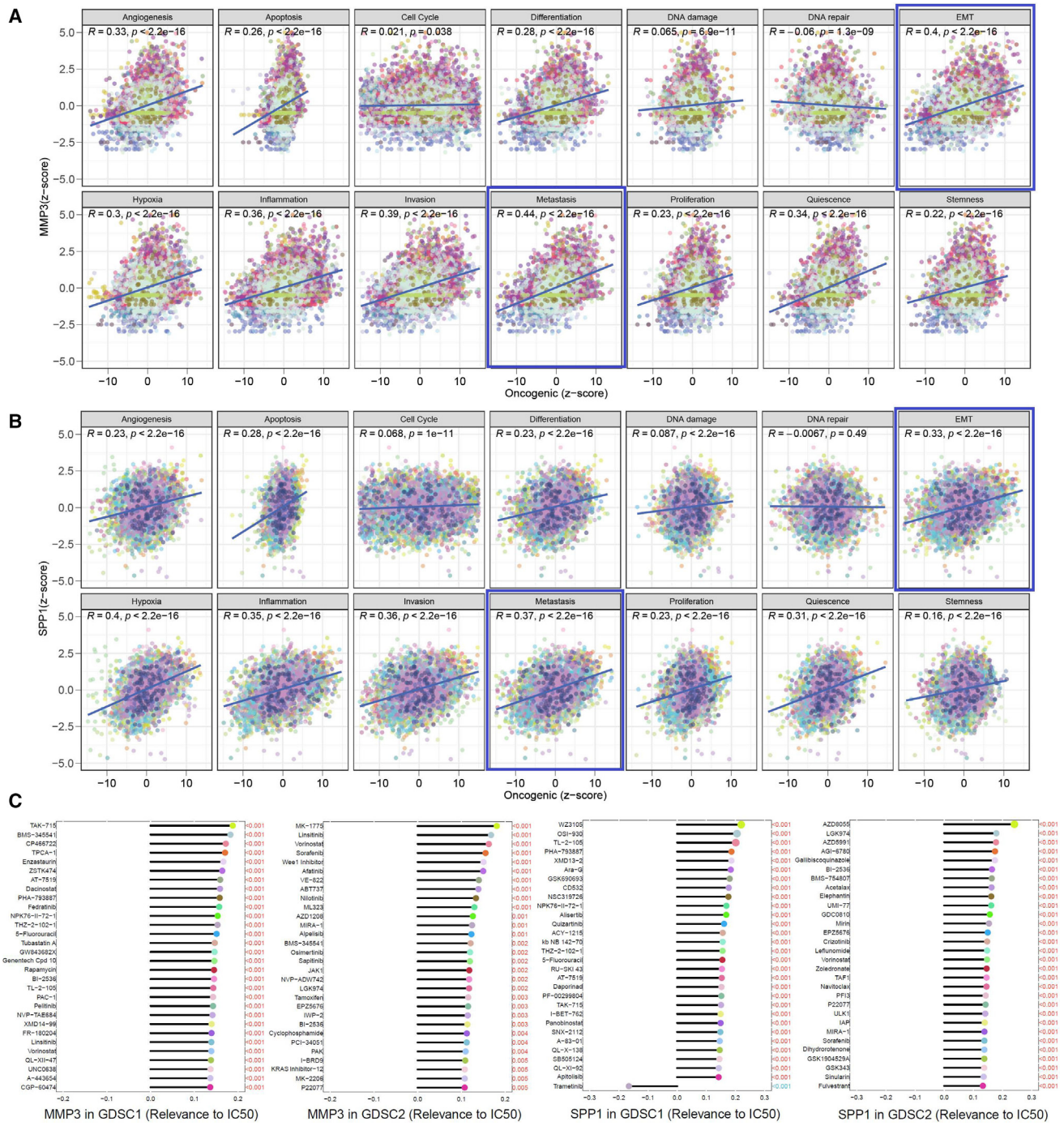

Figure 6. The participation of MMP3 and SPP1 in cell status and drug sensitivity across various tumor types

(A) Cell status analysis of MMP3 across various tumor types.

(B) Cell status analysis of SPP1 across various tumor types.

(C) Anti-tumor drug sensitivity analysis of MMP3 and SPP1.

MMP3 and SPP1 were similarly found to be significantly associated with the activation of EMT and the NF-κB signaling pathway in a comprehensive analysis of hallmark and metabolic pathways (Figures S3 and S4). The expression of MMP3 and SPP1 was positively correlated with the Half Maximal Inhibitory Concentration (IC50) values of various anti-tumor drugs, indicating that higher expression levels of MMP3 and SPP1 were associated with increased resistance to anti-tumor drugs (Figure 6C). These

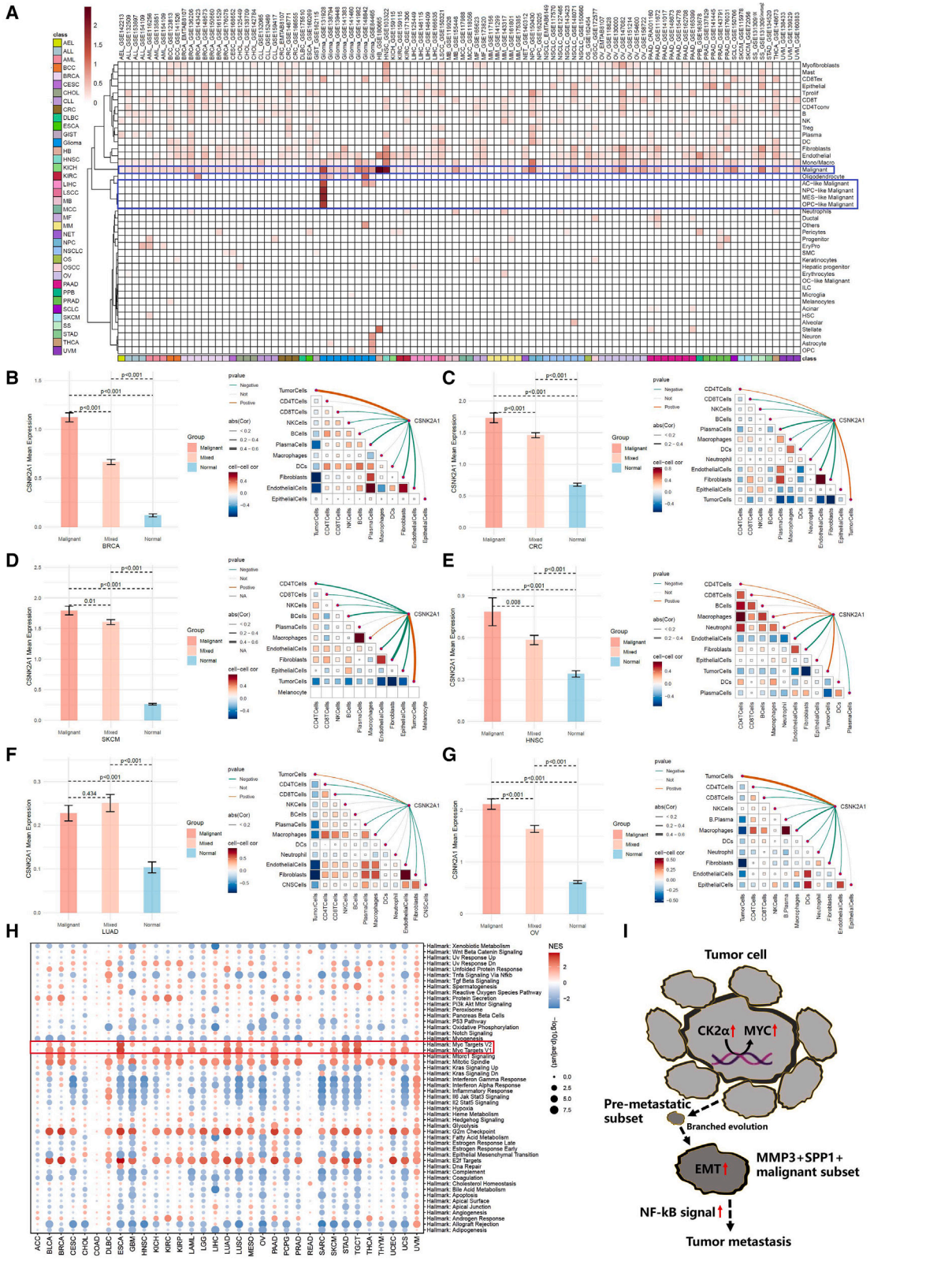

(legend on next page)

findings suggested that they may be potential factors contributing to the failure of chemotherapy or targeted therapy. All the evidence strongly suggested an association between MMP3 and SPP1 with adverse outcomes in tumor patients.

CK2α as an actionable therapeutic target in different tumor types

The presence of intratumor branched evolution and genomic mutations made it difficult for single-target therapies to comprehensively control tumor progression. Based on our prior experimental results, we found that CK2α exhibited increased gene transcription expression within the malignant components of penile carcinoma, indicating elevated phosphorylation levels. In the analysis of 98 pan-tumor single-cell datasets (Table S1), we unveiled that CK2α exhibited the highest expression intensity within the malignant components, echoing our findings in penile carcinoma (Figure 7A). This suggested that the elevation of phosphorylation levels within malignant cell subpopulations was a prevalent phenomenon across different types of malignant tumors. Spatial transcriptomics sequencing analysis across multiple tumors indicated a highly consistent localization of CK2α expression with previous pan-cancer single-cell results (Figures 7B–7G and S5). Moreover, the expression level of CK2α was significantly positively correlated with the abundance of tumor cells within the spots. Importantly, CK2α was found to have a significant association with the activation of the Myc Proto-Oncogene (MYC) oncogene (Figure 7H). Building on our previous research findings, we inferred an important insight into tumorigenesis and metastasis: upregulated CK2α mediated the activation of oncogenes, thereby promoting tumor development. Subsequently, through ongoing branching evolution, a subpopulation with robust metastatic capabilities emerged within the tumor, which we defined as the MMP3+ SPP1+ malignant subset. Compared to other malignant subpopulations, this group exhibited a higher capacity for EMT (Figure 7I). These evidences suggested that CK2α was a potent and promising target for tumor therapy.

Verifying the therapeutic effect of the CK2α inhibitor Silmitasertib on penile carcinoma

Our study conducted a series of cell phenotype assays related to Silmitasertib intervention, aiming to explore whether targeted inhibition of CK2α could effectively suppress the malignant behavior of penile carcinoma cells, thus paving the way for therapeutic interventions. The inhibition rate of Silmitasertib on Penl1 and LM156 cells was detected by Cell Counting Kit-8 (CCK-8) assay, and the IC50 was calculated. For Penl1 cells, the IC50 values are 26.6 μM at 24 h, 14.3 μM at 48 h, and 5.28 μM at 72 h. For LM156 cells, the IC50 values are 85.3 μM at 24 h, 40.8 μM at 48 h, and 6.66 μM at 72 h. Hence, the experimental drug intervention concentration for Penl1 was 5.3 μM Silmitasertib, and, for LM156, it was 6.7 μM Silmitasertib. In the CCK-8 assay, the decrease in optical density values observed in the Silmitasertib group, in comparison to the Normal control group (NC group), indicated that Silmitasertib effectively inhibited the proliferation ability of both Penl1 and LM156 cells (Figure 8A). In the cell-cycle assay, we observed that the Silmitasertib group exhibited a prolonged G1 phase and a reduced S phase in Penl1 and LM156 cells compared to the NC group (Figure 8B). In the apoptosis assay, compared to the NC group, Silmitasertib induced a higher apoptosis rate in Penl1 and LM156 cells, indicating that Silmitasertib could promote apoptosis in Penl1 and LM156 (Figure 8C). In the cell migration and invasion assays, Silmitasertib demonstrated a reduction in cell migration rate and invasive count compared to the NC group (Figures 8D and 8E). In the cell proliferation assay, it was confirmed that Silmitasertib disrupted the proliferation ability of Penl1 and LM156 cells, as evidenced by 5-Ethynyl-2'-deoxyuridine (EDU) staining (Figure 8F).

DISCUSSION

Intratumor heterogeneity laid the groundwork for nurturing tumor metastasis.[18,19] In the pre-metastasis process, the branching evolution of tumor cell subsets was accompanied by metabolic reprogramming and survival of the fittest.[20] The continuous accumulation of functional mutations and selective survival can lead to the emergence of malignant cells with high metastatic potential. These cells may gradually form dominant subpopulations and break through the burden of the immune surveillance system, thus marking the onset of metastasis.[21] Here, our study conducted single-cell analysis of advanced penile carcinoma, spatial transcriptomics analysis of squamous cell carcinoma (SCC), and bulk RNA-seq of twelve tumor samples to comprehensively dissect the heterogeneity within penile carcinoma. The MMP3+SPP1+ malignant subset was defined as a pre-metastatic subgroup in penile carcinoma. Based on the pseudo-time trajectory of cell development, the MMP3+SPP1+ malignant subset was notably distinguishable from other malignant subsets. Functionally, its two primary features were EMT and metastasis. Moreover, the signaling pathways it engaged in, specifically NF-κB and Toll-like receptor signaling pathways, were closely linked to lymph node metastasis in penile carcinoma. These findings brought to mind previous reports that showed MMP3 and SPP1's ability to promote metastasis in other tumors.[22–24] Additionally, the high phosphorylation was a significant biochemical characteristic of malignant cells in penile carcinoma ecology, and the CK2α inhibitor Silmitasertib showed significant inhibitory effects on penile tumor cell lines (Penl1 and LM156). Actually, our analysis of 98 single-cell transcriptomic datasets and 6 spatial transcriptomic datasets consistently revealed a significant upregulation of CK2α in the malignant components of various tumors. Therefore, we had ample evidence to propose that the MMP3+SPP1+ malignant subset

Figure 7. Single-cell and spatial transcriptomics sequencing dissect the transcriptional expression and localization of CK2α

(A) CK2α coding gene expression and localization were analyzed by 98 pan-tumor single-cell datasets.

(B–G) At spatial resolution, the Spearman correlation between the expression of the CK2α coding gene and the components of the microenvironment, as well as its expression differences in malignant, mixed, and normal regions. Data are represented as mean ± SD.

(H) Enrichment analysis of hallmark gene sets in high- and low-CK2α-expression groups across pan-cancer.

(I) Hypothesis of the overexpression of CK2α and the MMP3+SPP1+ pre-metastatic subpopulation in penile carcinoma.

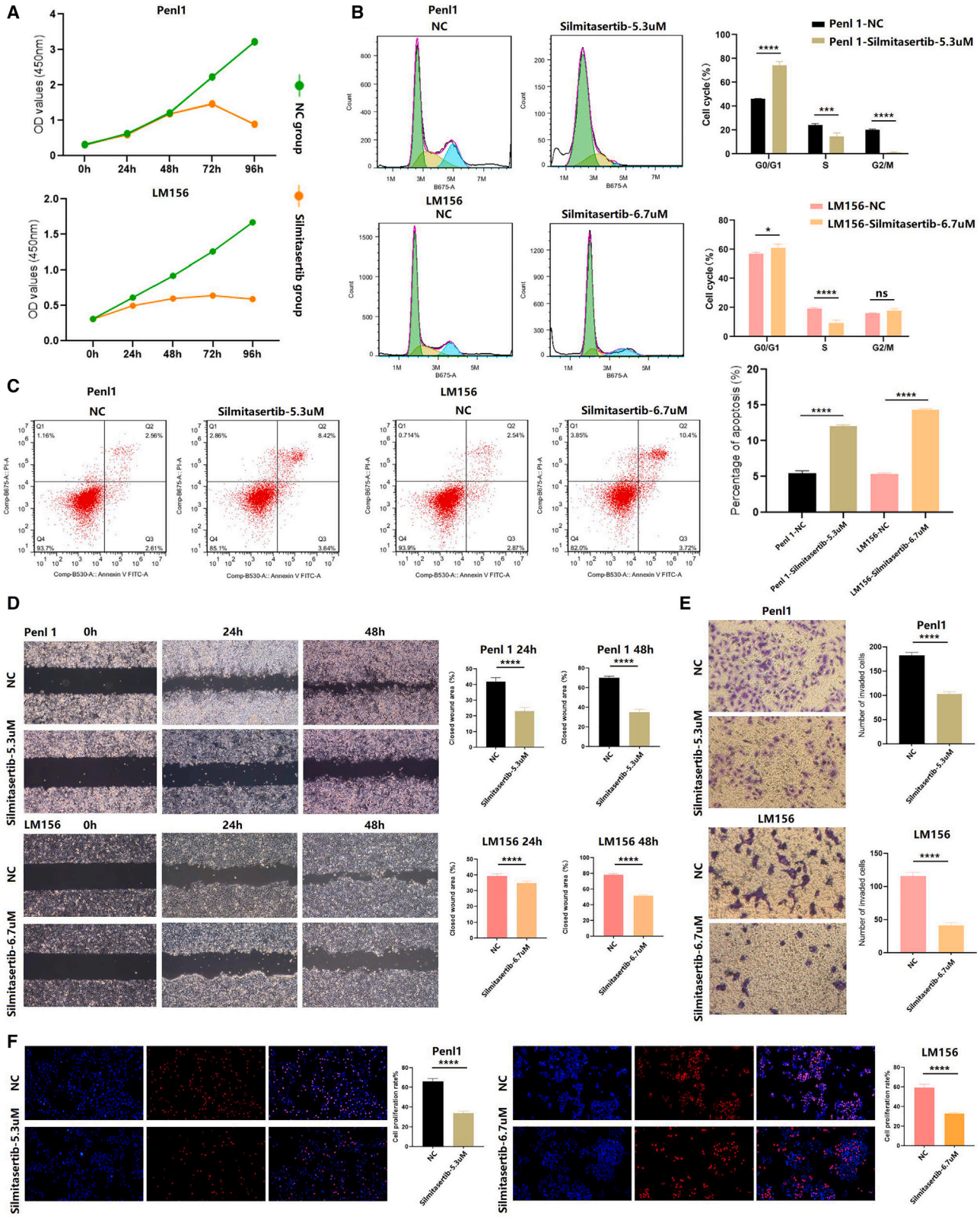

(legend on next page)

may serve as an adverse prognostic indicator in penile carcinoma patients, while CK2α could represent a promising therapeutic target.

Despite MMP3 and SPP1 being the major mediators of metastasis in many types of tumors,[25,26] there is currently no targeted inhibitor of them that has been successfully applied in clinical practice. Intratumor heterogeneity resulted in the inability of a single-targeted therapeutic drug to completely control disease progression.[27,28] Importantly, the excessive activation of phosphorylation signaling pathways was closely associated with the reshaping of intratumor heterogeneity and metabolic reprogramming, thereby increasing the likelihood of generating malignant subsets with a high potential for metastasis.[29–31] The enhanced phosphorylation of the NF-κB signaling pathway promoted tumor metastasis.[32–34] Overexpression of CK2α not only upregulated MYC but also enhanced the expression of EMT-related genes.[35] In our studies on penile carcinoma and pan-tumor, we confirmed the abundant presence of CK2α, MMP3, and SPP1. Based on these findings, we inferred that restricting CK2α expression could weaken tumor malignancy, making CK2α a potential vulnerability to target in penile carcinoma and other metastatic tumors. Silmitasertib is an anti-cancer drug that has been under exploration in recent years, and some preclinical studies have shown promising therapeutic effects in some tumors. Consequently, an increasing number of clinical trials involving Silmitasertib are being conducted in an orderly manner.[36,37] Our study represented the application report of Silmitasertib in penile carcinoma, expanding the range of its potential uses. The anti-tumor mechanism of Silmitasertib is currently mainly manifested in limiting the phosphorylation of oncogenic pathways,[38,39] reversing resistance to traditional chemotherapy,[40] sensitizing anti-tumor effect[41] and promoting tumor cell death,[42,43] and maintaining tumor suppressor molecules.[44] Our experiment emphasized the anti-tumor effect of Silmitasertib in penile carcinoma cells by inhibiting cell proliferation, invasion, and migration; blocking cell cycle; and promoting cell apoptosis. In short, we have presented groundbreaking evidence for the treatment of a rare genitourinary tumor with Silmitasertib.

Conclusion

Overall, our study presented significant advancements in understanding CK2α-mediated tumorigenesis and the MMP3+SPP1+ pre-metastatic subpopulation in penile carcinoma and other tumors. These findings provided valuable insights into the potential of Silmitasertib as a therapeutic agent.

Limitations of the study

Indeed, our study has some limitations. Due to the rarity and specificity of this disease, obtaining normal penile tissue and metastatic penile carcinoma tissue presents significant challenges. Currently, our focus is on developing penile carcinoma organoids and humanized mouse models. These models will serve to validate the findings from high-throughput sequencing of penile carcinoma, enhancing our understanding of the intricate relationships between the tumor, treatment modalities, and the microenvironment.

RESOURCE AVAILABILITY

Lead contact

Further information and requests for resources and reagents should be directed to and will be fulfilled by the lead contact, Miao Mo (momiao@hotmail.com).

Materials availability

This study did not generate new unique reagents.

Data and code availability

- Bulk RNA-seq data have been deposited in NCBI Sequence Read Archive and are publicly available as of the date of publication. Accession numbers are listed in the key resources table.
- This paper does not report original code.
- Any additional information required to reanalyze the data reported in this paper is available from the lead contact upon request.

ACKNOWLEDGMENTS

This study was supported by a grant from the National Natural Science Foundation of China (82103639).

AUTHOR CONTRIBUTIONS

D.-M.X.: investigation, formal analysis, writing – original draft, and writing – review and editing. L.-X.C.: investigation, supervision, and writing – original draft. H.H.: conceptualization and writing – review and editing. M.M.: conceptualization, project administration, and writing – review and editing.

DECLARATION OF INTERESTS

The authors declare no competing interests.

STAR★METHODS

Detailed methods are provided in the online version of this paper and include the following:

- KEY RESOURCES TABLE
- EXPERIMENTAL MODEL AND STUDY PARTICIPANT DETAILS
- METHOD DETAILS
  - scRNA-seq analysis
  - Cell communication analysis
  - Cell status evaluation
  - Trajectory analysis
  - Functional enrichment analysis
  - Bulk RNA-seq analysis

Figure 8. Cell phenotype assays of Penl1 and LM156 cells in both the negative control group and the Silmitasertib group

(A) CCK-8 assay.
(B) Cell-cycle assay.
(C) Cell apoptosis assay.
(D) Cell migration assay.
(E) Cell invasion assay.
(F) EDU assay.
$^{*}p < 0.05$, $^{**}p < 0.01$, $^{***}p < 0.001$, $^{****}p < 0.0001$. All data are represented as mean ± SD.

SUPPLEMENTAL INFORMATION

Supplemental information can be found online at https://doi.org/10.1016/j.isci.2025.111765.

Received: July 15, 2024
Revised: September 28, 2024
Accepted: January 6, 2025
Published: January 7, 2025

REFERENCES

1. Gerlinger, M., Rowan, A.J., Horswell, S., Math, M., Larkin, J., Endesfelder, D., Gronroos, E., Martinez, P., Matthews, N., Stewart, A., et al. (2012). Intratumor heterogeneity and branched evolution revealed by multiregion sequencing. N. Engl. J. Med. *366*, 883–892. https://doi.org/10.1056/NEJMoa1113205.
2. Hunter, K.W., Amin, R., Deasy, S., Ha, N.H., and Wakefield, L. (2018). Genetic insights into the morass of metastatic heterogeneity. Nat. Rev. Cancer *18*, 211–223. https://doi.org/10.1038/nrc.2017.126.
3. Caswell, D.R., and Swanton, C. (2017). The role of tumour heterogeneity and clonal cooperativity in metastasis, immune evasion and clinical outcome. BMC Med. *15*, 133. https://doi.org/10.1186/s12916-017-0900-y.
4. Sachdeva, A., McGuinness, L., Zapala, Ł., Greco, I., Garcia-Perdomo, H.A., Kailavasan, M., Antunes-Lopes, T., Ayres, B., Barreto, L., Campi, R., et al. (2024). Management of Lymph Node-positive Penile Cancer: A Systematic Review. Eur. Urol. *85*, 257–273. https://doi.org/10.1016/j.eururo.2023.04.018.
5. Pagliaro, L.C., Williams, D.L., Daliani, D., Williams, M.B., Osai, W., Kincaid, M., Wen, S., Thall, P.F., and Pettaway, C.A. (2010). Neoadjuvant paclitaxel, ifosfamide, and cisplatin chemotherapy for metastatic penile cancer: a phase II study. J. Clin. Oncol. *28*, 3851–3857. https://doi.org/10.1200/JCO.2010.29.5477.
6. Correia, A.L., Mori, H., Chen, E.I., Schmitt, F.C., and Bissell, M.J. (2013). The hemopexin domain of MMP3 is responsible for mammary epithelial invasion and morphogenesis through extracellular interaction with HSP90β. Genes Dev. *27*, 805–817. https://doi.org/10.1101/gad.211383.112.
7. Seehawer, M., Li, Z., Nishida, J., Foidart, P., Reiter, A.H., Rojas-Jimenez, E., Goyette, M.A., Yan, P., Raval, S., Munoz Gomez, M., et al. (2024). Loss of Kmt2c or Kmt2d drives brain metastasis via KDM6A-dependent upregulation of MMP3. Nat. Cell Biol. *26*, 1165–1175. https://doi.org/10.1038/s41556-024-01446-3.
8. Deng, G., Zeng, F., Su, J., Zhao, S., Hu, R., Zhu, W., Hu, S., Chen, X., and Yin, M. (2020). BET inhibitor suppresses melanoma progression via the noncanonical NF-κB/SPP1 pathway. Theranostics *10*, 11428–11443. https://doi.org/10.7150/thno.47432.
9. Trembley, J.H., Wang, G., Unger, G., Slaton, J., and Ahmed, K. (2009). Protein kinase CK2 in health and disease: CK2: a key player in cancer biology. Cell. Mol. Life Sci. *66*, 1858–1867. https://doi.org/10.1007/s00018-009-9154-y.
10. Roffey, S.E., and Litchfield, D.W. (2021). CK2 Regulation: Perspectives in 2021. Biomedicines *9*, 1361. https://doi.org/10.3390/biomedicines9101361.
11. Borgo, C., D'Amore, C., Sarno, S., Salvi, M., and Ruzzene, M. (2021). Protein kinase CK2: a potential therapeutic target for diverse human diseases. Signal Transduct. Targeted Ther. *6*, 183. https://doi.org/10.1038/s41392-021-00567-7.
12. Tawfic, S., Yu, S., Wang, H., Faust, R., Davis, A., and Ahmed, K. (2001). Protein kinase CK2 signal in neoplasia. Histol. Histopathol. *16*, 573–582. https://doi.org/10.14670/HH-16.573.
13. Hanahan, D., and Weinberg, R.A. (2011). Hallmarks of cancer: the next generation. Cell *144*, 646–674. https://doi.org/10.1016/j.cell.2011.02.013.
14. Hanahan, D. (2022). Hallmarks of Cancer: New Dimensions. Cancer Discov. *12*, 31–46. https://doi.org/10.1158/2159-8290.CD-21-1059.
15. Garusi, E., Rossi, S., and Perris, R. (2012). Antithetic roles of proteoglycans in cancer. Cell. Mol. Life Sci. *69*, 553–579. https://doi.org/10.1007/s00018-011-0816-1.
16. Mirzaei, S., Saghari, S., Bassiri, F., Raesi, R., Zarrabi, A., Hushmandi, K., Sethi, G., and Tergaonkar, V. (2022). NF-κB as a regulator of cancer metastasis and therapy response: A focus on epithelial-mesenchymal transition. J. Cell. Physiol. *237*, 2770–2795. https://doi.org/10.1002/jcp.30759.
17. Khajeh Alizadeh Attar, M., Anwar, M.A., Eskian, M., Keshavarz-Fathi, M., Choi, S., and Rezaei, N. (2018). Basic understanding and therapeutic approaches to target toll-like receptors in cancerous microenvironment and metastasis. Med. Res. Rev. *38*, 1469–1484. https://doi.org/10.1002/med.21480.
18. Scheele, C.L.G.J., Maynard, C., and van Rheenen, J. (2016). Intravital Insights into Heterogeneity, Metastasis, and Therapy Responses. Trends Cancer *2*, 205–216. https://doi.org/10.1016/j.trecan.2016.03.001.
19. Gerstberger, S., Jiang, Q., and Ganesh, K. (2023). Metastasis. Cell *186*, 1564–1579. https://doi.org/10.1016/j.cell.2023.03.003.
20. Raskov, H., Gaggar, S., Tajik, A., Orhan, A., and Gögenur, I. (2023). Metabolic switch in cancer – Survival of the fittest. Eur. J. Cancer *180*, 30–51. https://doi.org/10.1016/j.ejca.2022.11.025.
21. Gonzalez, H., Hagerling, C., and Werb, Z. (2018). Roles of the immune system in cancer: from tumor initiation to metastatic progression. Genes Dev. *32*, 1267–1284. https://doi.org/10.1101/gad.314617.118.
22. Dai, W., Guo, C., Wang, Y., Li, Y., Xie, R., Wu, J., Yao, B., Xie, D., He, L., Li, Y., et al. (2023). Identification of hub genes and pathways in lung metastatic colorectal cancer. BMC Cancer *23*, 323. https://doi.org/10.1186/s12885-023-10792-8.
23. He, L., Kang, Q., Chan, K.I., Zhang, Y., Zhong, Z., and Tan, W. (2022). The immunomodulatory role of matrix metalloproteinases in colitis-associated cancer. Front. Immunol. *13*, 1093990. https://doi.org/10.3389/fimmu.2022.1093990.
24. Wu, J., Shen, Y., Zeng, G., Liang, Y., and Liao, G. (2024). SPP1+ TAM subpopulations in tumor microenvironment promote intravasation and metastasis of head and neck squamous cell carcinoma. Cancer Gene Ther. *31*, 311–321. https://doi.org/10.1038/s41417-023-00704-0.
25. Chu, C., Liu, X., Bai, X., Zhao, T., Wang, M., Xu, R., Li, M., Hu, Y., Li, W., Yang, L., et al. (2018). MiR-519d suppresses breast cancer tumorigenesis and metastasis via targeting MMP3. Int. J. Biol. Sci. *14*, 228–236. https://doi.org/10.7150/ijbs.22849.
26. Pang, X., Xie, R., Zhang, Z., Liu, Q., Wu, S., and Cui, Y. (2019). Identification of SPP1 as an Extracellular Matrix Signature for Metastatic Castration-Resistant Prostate Cancer. Front. Oncol. *9*, 924. https://doi.org/10.3389/fonc.2019.00924.
27. Huang, T., Song, X., Xu, D., Tiek, D., Goenka, A., Wu, B., Sastry, N., Hu, B., and Cheng, S.Y. (2020). Stem cell programs in cancer initiation, progression, and therapy resistance. Theranostics *10*, 8721–8743. https://doi.org/10.7150/thno.41648.
28. Park, J.H., Pyun, W.Y., and Park, H.W. (2020). Cancer Metabolism: Phenotype, Signaling and Therapeutic Targets. Cells *9*, 2308. https://doi.org/10.3390/cells9102308.

29. Liu, Z., Liu, Y., Qian, L., Jiang, S., Gai, X., Ye, S., Chen, Y., Wang, X., Zhai, L., Xu, J., et al. (2021). A proteomic and phosphoproteomic landscape of KRAS mutant cancers identifies combination therapies. Mol. Cell *81*, 4076–4090.e8. https://doi.org/10.1016/j.molcel.2021.07.021.

30. Uslu, C., Kapan, E., and Lyakhovich, A. (2024). Cancer resistance and metastasis are maintained through oxidative phosphorylation. Cancer Lett. *587*, 216705. https://doi.org/10.1016/j.canlet.2024.216705.

31. Esparza-Moltó, P.B., and Cuezva, J.M. (2020). Reprogramming Oxidative Phosphorylation in Cancer: A Role for RNA-Binding Proteins. Antioxidants Redox Signal. *33*, 927–945. https://doi.org/10.1089/ars.2019.7988.

32. Rong, D., Sun, G., Zheng, Z., Liu, L., Chen, X., Wu, F., Gu, Y., Dai, Y., Zhong, W., Hao, X., et al. (2022). MGP promotes CD8+ T cell exhaustion by activating the NF-κB pathway leading to liver metastasis of colorectal cancer. Int. J. Biol. Sci. *18*, 2345–2361. https://doi.org/10.7150/ijbs.70137.

33. Jiao, J., Ruan, L., Cheng, C.S., Wang, F., Yang, P., and Chen, Z. (2023). Paired protein kinases PRKCI-RIPK2 promote pancreatic cancer growth and metastasis via enhancing NF-κB/JNK/ERK phosphorylation. Mol. Med. *29*, 47. https://doi.org/10.1186/s10020-023-00648-z.

34. Liu, B., Sun, L., Liu, Q., Gong, C., Yao, Y., Lv, X., Lin, L., Yao, H., Su, F., Li, D., et al. (2015). A cytoplasmic NF-κB interacting long noncoding RNA blocks IκB phosphorylation and suppresses breast cancer metastasis. Cancer Cell *27*, 370–381. https://doi.org/10.1016/j.ccell.2015.02.004.

35. Zou, J., Luo, H., Zeng, Q., Dong, Z., Wu, D., and Liu, L. (2011). Protein kinase CK2α is overexpressed in colorectal cancer and modulates cell proliferation and invasion via regulating EMT-related genes. J. Transl. Med. *9*, 97. https://doi.org/10.1186/1479-5876-9-97.

36. Salvi, M., Borgo, C., Pinna, L.A., and Ruzzene, M. (2021). Targeting CK2 in cancer: a valuable strategy or a waste of time? Cell Death Dis. *7*, 325. https://doi.org/10.1038/s41420-021-00717-4.

37. D'Amore, C., Borgo, C., Sarno, S., and Salvi, M. (2020). Role of CK2 inhibitor CX-4945 in anti-cancer combination therapy – potential clinical relevance. Cell. Oncol. *43*, 1003–1016. https://doi.org/10.1007/s13402-020-00566-w.

38. Solaipriya, S., Anbalagan, M., and Sivaramakrishnan, V. (2024). Preclinical Targeting of the PGRMC1-CK2 Axis with Silmitasertib: A Potential Strategy for Lung Adenocarcinoma Therapy. Drug Res. *74*, 187–190. https://doi.org/10.1055/a-2273-2389.

39. Guo, Y., Zhu, Z., Huang, Z., Cui, L., Yu, W., Hong, W., Zhou, Z., Du, P., and Liu, C.Y. (2022). CK2-induced cooperation of HHEX with the YAP-TEAD4 complex promotes colorectal tumorigenesis. Nat. Commun. *13*, 4995. https://doi.org/10.1038/s41467-022-32674-6.

40. Liu, Z.D., Shi, Y.H., Xu, Q.C., Zhao, G.Y., Zhu, Y.Q., Li, F.X., Ma, M.J., Ye, J.Y., Huang, X.T., Wang, X.Y., et al. (2024). CSNK2A1 confers gemcitabine resistance to pancreatic ductal adenocarcinoma via inducing autophagy. Cancer Lett. *585*, 216640. https://doi.org/10.1016/j.canlet.2024.216640.

41. Thus, Y.J., De Rooij, M.F.M., Swier, N., Beijersbergen, R.L., Guikema, J.E.J., Kersten, M.J., Eldering, E., Pals, S.T., Kater, A.P., and Spaargaren, M. (2023). Inhibition of casein kinase 2 sensitizes mantle cell lymphoma to venetoclax through MCL-1 downregulation. Haematologica *108*, 797–810. https://doi.org/10.3324/haematol.2022.281668.

42. Wang, S., Yadav, A.K., Han, J.Y., Ahn, K.S., and Jang, B.C. (2022). Anti-Growth, Anti-Angiogenic, and Pro-Apoptotic Effects by CX-4945, an Inhibitor of Casein Kinase 2, on HuCCT-1 Human Cholangiocarcinoma Cells via Control of Caspase-9/3, DR-4, STAT-3/STAT-5, Mcl-1, eIF-2α, and HIF-1α. Int. J. Mol. Sci. *23*, 6353. https://doi.org/10.3390/ijms23116353.

43. Bancet, A., Frem, R., Jeanneret, F., Mularoni, A., Bazelle, P., Roelants, C., Delcros, J.G., Guichou, J.F., Pillet, C., Coste, I., et al. (2024). Cancer selective cell death induction by a bivalent CK2 inhibitor targeting the ATP site and the allosteric αD pocket. iScience *27*, 108903. https://doi.org/10.1016/j.isci.2024.108903.

44. Hermosilla, V.E., Gyenis, L., Rabalski, A.J., Armijo, M.E., Sepúlveda, P., Duprat, F., Benítez-Riquelme, D., Fuentes-Villalobos, F., Quiroz, A., Hepp, M.I., et al. (2024). Casein kinase 2 phosphorylates and induces the SALL2 tumor suppressor degradation in colon cancer cells. Cell Death Dis. *15*, 223. https://doi.org/10.1038/s41419-024-06591-z.

45. Zhou, Q.H., Deng, C.Z., Li, Z.S., Chen, J.P., Yao, K., Huang, K.B., Liu, T.Y., Liu, Z.W., Qin, Z.K., Zhou, F.J., et al. (2018). Molecular characterization and integrative genomic analysis of a panel of newly established penile cancer cell lines. Cell Death Dis. *9*, 684. https://doi.org/10.1038/s41419-018-0736-1.

46. Xu, D.M., Zhuang, X.Y., Ma, H.L., Li, Z.S., Wei, L.C., Luo, J.H., and Han, H. (2024). Altered tumor microenvironment heterogeneity of penile cancer during progression from non-lymphatic to lymphatic metastasis. Cancer Med. *13*, e70025. https://doi.org/10.1002/cam4.70025.

47. Lun, A.T.L., Riesenfeld, S., Andrews, T., Dao, T.P., Gomes, T., and participants in the 1st Human Cell Atlas Jamboree; and Marioni, J.C. (2019). EmptyDrops: distinguishing cells from empty droplets in droplet-based single-cell RNA sequencing data. Genome Biol. *20*, 63. https://doi.org/10.1186/s13059-019-1662-y.

48. Butler, A., Hoffman, P., Smibert, P., Papalexi, E., and Satija, R. (2018). Integrating single-cell transcriptomic data across different conditions, technologies, and species. Nat. Biotechnol. *36*, 411–420. https://doi.org/10.1038/nbt.4096.

49. Korsunsky, I., Millard, N., Fan, J., Slowikowski, K., Zhang, F., Wei, K., Baglaenko, Y., Brenner, M., Loh, P.R., and Raychaudhuri, S. (2019). Fast, sensitive and accurate integration of single-cell data with Harmony. Nat. Methods *16*, 1289–1296. https://doi.org/10.1038/s41592-019-0619-0.

50. Jin, S., Guerrero-Juarez, C.F., Zhang, L., Chang, I., Ramos, R., Kuan, C.H., Myung, P., Plikus, M.V., and Nie, Q. (2021). Inference and analysis of cell-cell communication using CellChat. Nat. Commun. *12*, 1088. https://doi.org/10.1038/s41467-021-21246-9.

51. Yuan, H., Yan, M., Zhang, G., Liu, W., Deng, C., Liao, G., Xu, L., Luo, T., Yan, H., Long, Z., et al. (2019). CancerSEA: a cancer single-cell state atlas. Nucleic Acids Res. *47*, D900–D908. https://doi.org/10.1093/nar/gky939.

52. Trapnell, C., Cacchiarelli, D., Grimsby, J., Pokharel, P., Li, S., Morse, M., Lennon, N.J., Livak, K.J., Mikkelsen, T.S., and Rinn, J.L. (2014). The dynamics and regulators of cell fate decisions are revealed by pseudotemporal ordering of single cells. Nat. Biotechnol. *32*, 381–386. https://doi.org/10.1038/nbt.2859.

53. Wolf, F.A., Hamey, F.K., Plass, M., Solana, J., Dahlin, J.S., Göttgens, B., Rajewsky, N., Simon, L., and Theis, F.J. (2019). PAGA: graph abstraction reconciles clustering with trajectory inference through a topology preserving map of single cells. Genome Biol. *20*, 59. https://doi.org/10.1186/s13059-019-1663-x.

54. Ashburner, M., Ball, C.A., Blake, J.A., Botstein, D., Butler, H., Cherry, J.M., Davis, A.P., Dolinski, K., Dwight, S.S., Eppig, J.T., et al. (2000). Gene ontology: tool for the unification of biology. The Gene Ontology Consortium. Nat. Genet. *25*, 25–29. https://doi.org/10.1038/75556.

55. Kanehisa, M., and Goto, S. (2000). KEGG: yoto encyclopedia of genes and genomes. Nucleic Acids Res. *28*, 27–30. https://doi.org/10.1093/nar/28.1.27.

56. Subramanian, A., Tamayo, P., Mootha, V.K., Mukherjee, S., Ebert, B.L., Gillette, M.A., Paulovich, A., Pomeroy, S.L., Golub, T.R., Lander, E.S., and Mesirov, J.P. (2005). Gene set enrichment analysis: a knowledge-based approach for interpreting genome-wide expression profiles. Proc. Natl. Acad. Sci. USA *102*, 15545–15550. https://doi.org/10.1073/pnas.0506580102.

57. Meyers, R.M., Bryan, J.G., McFarland, J.M., Weir, B.A., Sizemore, A.E., Xu, H., Dharia, N.V., Montgomery, P.G., Cowley, G.S., Pantel, S., et al. (2017). Computational correction of copy number effect improves specificity of CRISPR-Cas9 essentiality screens in cancer cells. Nat. Genet. *49*, 1779–1784. https://doi.org/10.1038/ng.3984.

STAR★METHODS

KEY RESOURCES TABLE

REAGENT or RESOURCE	SOURCE	IDENTIFIER
Biological samples		
Penile carcinoma tissues	Sun Yat-sen University Cancer Center	N/A
Critical commercial assays		
CCK8	Suzhou Youyi Landi Biotechnology Co., Ltd	C6005M
Silmitasertib	MedChemExpress(MCE)	CX-4945
Deposited data		
Bulk RNA-seq of penile carcinoma and metastatic lymph nodes	NCBI Sequence Read Archive	BioProject ID: PRJNA1193573
Single-cell data of penile carcinoma	Xu et al. study	https://doi.org/10.1002/cam4.70025
Bulk RNA-seq of penile carcinoma	Gene Expression Omnibus	GSE196978
Spatial transcriptomics data of squamous cell carcinoma	Gene Expression Omnibus	GSE144239
RNA-seq of pan-tumor	TCGA Genomic Data Commons	https://portal.gdc.cancer.gov/
Pan-tumor single-cell datasets	TISCH2	https://doi.org/10.1093/nar/gkac959
Experimental models: Cell lines		
Penl 1	Sun Yat-sen University Cancer Center[45]	N/A
LM156	Sun Yat-sen University Cancer Center[45]	N/A
Software and algorithms		
R software	the R Core Team and the R Foundation for Statistical Computing	version 4.3.3
GraphPad Prism 5 software	GraphPad Software, Inc.	https:www.graphpad.com/scientificsoftware/prism
Cell Ranger	10x Genomics	https://doi.org/10.1186/s13059-019-1662-y
Seurat	https://satijalab.org/seurat/	https://doi.org/10.1038/nbt.4096
CellChat	Github	https://github.com/sqjin/CellChat
Monocle	Github	http://cole-trapnelllab.github.io/monoclerelease
GSVA	Github	https://github.com/rcastelo/GSVA

EXPERIMENTAL MODEL AND STUDY PARTICIPANT DETAILS

We collected twelve tumor samples from six advanced-stage penile carcinoma patients (Table S2), comprising six primary lesions and six metastatic lymph nodes, which were used for bulk RNA-seq. These specimens were pathologically confirmed as squamous cell carcinoma of the penis and there were no significant differences in age and HPV infection status among the patients. Prior to obtaining tumor samples, all patients had no history of anti-tumor therapy. Additionally, four public single-cell RNA sequencing (scRNA-seq) datasets from patients with advanced-stage penile carcinoma[46] and two spatial transcriptomics datasets of SCC (GSE144239) were also included in this analysis.

This research was approved by the Institutional Review Board of Sun Yat-sen University Cancer Center (B2023-390-01) and conducted in accordance with the criteria set by the Declaration of Helsinki. The study design and conduct complied with all relevant regulations regarding the use of human study participants. All patients signed written informed consent.

METHOD DETAILS

scRNA-seq analysis

Cell Ranger[47] and Seurat[48] were utilized for cell identification and gene expression analysis in single-cell data. The gene count per single cell was set between 500 and 3000, with the mitochondrial gene expression accounting for less than 20%. Harmony was used to correct batch effects.[49]

Cell communication analysis

CellChat was utilized for analyzing the cellular communication network between different immune cell subtypes and different malignant cell subtypes, as well as predicting signaling pathways between ligand and receptor.[50]

Cell status evaluation

CancerSEA database was used to score the cell status of malignant cell subsets by evaluating the expression levels of marker genes, aiming to identify the subset with the highest metastatic potential.[51]

Trajectory analysis

Monocle utilized gene expression data to construct single-cell trajectories, thereby inferring the evolution of cell subsets along a pseudo-time axis.[52] PAGA trajectory analysis further inferred the potential connections between cell subpopulations along a pseudo-time axis.[53]

Functional enrichment analysis

GO[54] and KEGG[55] enrichment analyses were employed to elucidate the signaling pathways and cellular functional characteristics in MMP3+SPP1+ malignant subset. Gene set enrichment analysis (GSEA)[56] enrichment analysis was utilized to unveil the differences in signaling pathways at the bulk transcriptomic level between metastatic lymph nodes and primary penile carcinoma.

Bulk RNA-seq analysis

Bulk RNA-seq experiments of twelve tumor samples, including six primary penile carcinoma and six metastatic lymph nodes were conducted to assess the variations in gene expression between penile carcinoma and metastatic lymph nodes. The public dataset GSE196978 was used to validate the expression of MMP3 and SPP1 in penile carcinoma and normal penis.

Pan-tumor study

The PanCanAtlas TCGA project provided normalized RNA-seq datasets that can be used to investigate the expression patterns of MMP3 and SPP1 genes across different types of tumors.

The DepMap database provided whole-genome CRISPR-Cas9 screening scores for pan-tumor cell line essentiality, using the CERES algorithm.[57] These scores can help infer the effect of PTGS2 gene knockout on cell growth.

The seven-algorithm pan-tumor immune infiltration analysis was used to comprehensively reveal the correlation between MMP3 and immune-infiltrating cells, including algorithms CIBERSORT, CIBERSORT-ABS, XCELL, EPIC, MCPCOUNTER, QUANTISEQ and TIMER.

In hallmark and metabolism analysis of pan-tumor, MMP3 and SPP1 were evaluated for their association with 50 hallmark gene sets and 85 metabolic gene sets by clusterProfiler package. In the pathway disturbance analysis, we evaluated the effects of MMP3 and SPP1 on the NF-κB signaling pathway using the PROGENy algorithm from the easier package. In cancer cell state analysis of pan-tumor, the *Z* score algorithm in the R package GSVA was utilized to compute 14 functional state gene sets. Pearson correlation analysis was then employed to determine the correlation between target genes and the Z-scores of each functional gene sets.

Analyzing 98 pan-tumor single-cell datasets was a comprehensive approach to identify the transcriptional expression of CK2α (Coding gene: CSNK2A1), enabling us to infer which cellular subpopulations it was active in. The pheatmap package was employed to generate a heatmap visualization depicting the pan-tumor single-cell expression landscape of targeted gene.

Spatial transcriptomics sequencing maximized the acquisition of cellular spatial positioning information and gene expression data, thereby furthering research into the authentic gene expression profiles of cells within tissues. We incorporated spatial transcriptomics datasets from two SCC and other six different tumors published in the public domain to further validate the relationship between CK2α and malignant cell subsets within tumors.

Determination of IC50 values for Silmitasertib (Synonyms: CX-4945)

Silmitasertib was purchased from MedChemExpress Biotech Co., Ltd. (Monmouth Junction, NJ, USA). Penile carcinoma cell lines[45] (Penl1 and LM156 cells) were inoculated into a 96-well plate, then DMEM culture medium (Gibco, CA, USA) was added. In the drug treatment experiment, we established a control group (A) and experimental groups (B: 0.5μM Silmitasertib, C: 1μM Silmitasertib, D: 2μM Silmitasertib, E: 4μM Silmitasertib, F: 8μM Silmitasertib and G:16 μM Silmitasertib). The absorbance values of the cells were detected by cell counting kit-8 (CCK-8) method.

CCK-8 assay

CCK-8 assay was utilized to assess the proliferation of Penl1 and LM156 cells in both the negative control (NC) group and the Silmitasertib group. Penl1 cells were divided into control and experimental groups, with a final concentration of 5.3μM Silmitasertib in the experimental group. LM156 cells were also divided into control and experimental groups, with a final concentration of 6.7μM Silmitasertib in the experimental group. The CCK-8 assay was used to measure the absorbance values of these cells to assess their proliferation.

Cell cycle assay

The cells from the Penl1-NC group, Penl1-Silmitasertib-5.3μM group, LM156-NC group, and LM156-Silmitasertib-6.7μM group were centrifuged, washed, and resuspended to obtain single-cell suspensions, respectively. The PI staining (COOLABER, Beijing, China) was used to detect the changes in the cell cycle of Penl1 and LM156 cells before and after drug intervention. Red fluorescence was detected at 488nm excitation wavelength by flow cytometry.

Apoptosis assay

Cell apoptosis was detected to examine the influence of Silmitasertib on tumor cell apoptosis. Penl1 cells and LM156 cells were respectively divided into Penl1-NC group, Penl1-Silmitasertib-5.3μM group, LM156-NC group, and LM156-Silmitasertib-6.7μM group. Annexin V-FITC (Beyotime, Shanghai, China) and propidium iodide staining solutions were added to each group, followed by flow cytometry analysis of the samples.

Cell migration assay

The cells of the NC group and Silmitasertib-5.3μM group of Penl1, as well as the cells of the NC group and Silmitasertib-6.7μM group of LM56, were seeded into a 6-well plate and supplemented with culture medium. Cell scratching was performed when the cell confluence reached more than 95%. The cell migration at 0h, 24h and 48h was recorded.

Cell invasion assays

Matrigel (Corning, NY) was hydrated overnight at 4°C, diluted, and then applied as a coating in the transwell chamber (Costar, Cambridge, MA). Cell suspensions for the Penl1-NC group, Penl1-Silmitasertib-5.3μM group, LM156-NC group, and LM156-Silmitasertib-6.7μM group were prepared and seeded into the matrigel-coated invasion chambers. The cells were fixed with 4% paraformaldehyde (Coolaber, Beijing, China) for 20 min and then stained in crystal violet solution (Amresco Inc., USA) for 20 min. Afterward, they were rinsed with deionized water until the background was clear, and then photographed and analyzed.

EDU assay

After digesting the Penl-1 cell's NC group and Silmitasertib-5.3μM group, as well as the LM56 cell's NC group and Silmitasertib-6.3μM group, cell counting was performed. The cell density was adjusted to 5×10^5 cells/ml and added to a 6-well plate with a final volume of 2mL per well. The EDU working solution (Beyotime, Shanghai, China) was prepared, and the cells were incubated and washed. Hoechst 33342 (Sigma Chemical, St Louis, MO) was added to the mixture and incubate at room temperature in the dark. Following the aspiration and washing steps, qualitative analysis was conducted using a fluorescence microscope.

QUANTIFICATION AND STATISTICAL ANALYSIS

This study employed the Student's t test to analyze the data from cell functional experiments. Additionally, the Kruskal-Wallis test was utilized for comparisons involving multiple groups. IC50 values were calculated using GraphPad Prism 5 software. The significance threshold for both tests was set at $p < 0.05$. All analyses were conducted using R software version 4.3.3.